Silvana M. Azcarate[1]
Adriano de Araújo Gomes[2]
Luciana Vera-Candioti[3]
Mário Cesar Ugulino de Araújo[2]
José M. Camiña[1]*
Héctor C. Goicoechea[3]

[1]Facultad de Ciencias Exactas y Naturales, Universidad Nacional de La Pampa and Instituto de Ciencias de la Tierra y Ambientales de La Pampa (INCITAP), Santa Rosa, La Pampa, Argentina
[2]Laboratório de Automação e Instrumentação em Química Analítica e Quimiometria (LAQA), Universidade Federal da Paraíba, CCEN, Departamento de Química, João Pessoa, PB, Brasil
[3]Universidad Nacional del Litoral, CONICET, FBCB, Laboratorio de Desarrollo Analítico y Quimiometría (LADAQ), Ciudad Universitaria, 3000, Santa Fe, Argentina

Received February 1, 2016
Revised March 10, 2016
Accepted March 20, 2016

Research Article

Second-order capillary electrophoresis diode array detector data modeled with the Tucker3 algorithm: A novel strategy for Argentinean white wine discrimination respect to grape variety

Data obtained by capillary electrophoresis with diode array detection (CE-DAD) were modeled with the purpose to discriminate Argentinean white wines samples produced from three grape varieties (Torrontés, Chardonnay, and Sauvignon blanc). Thirty-eight samples of commercial white wine from four wine-producing provinces of Argentina (Mendoza, San Juan, Salta, and Rio Negro) were analyzed. CE-DAD matrices with dimensions of 421 elution times (from 1.17 to 7.39 minutes) × 71 wavelengths (from 227 to 367 nm) were joined in a three way data array and decomposed by Tucker3 method under non-negativity constraint, employing 18, 18 and six factors in the modes 1, 2 and 3, respectively. Using the scores of Tucker model, it was possible to discriminate samples of Argentinean white wine by linear discriminant analysis and Kernel linear discriminant analysis. Core element analysis of the Tucker3 model allows identifying the loading profiles in spectral mode related to Argentinean white wine samples.

Keywords:
Argentinean white wine / Capillary electrophoresis / LDA / Tucker3
DOI 10.1002/elps.201600052

1 Introduction

The wine composition varies depending of the grape type used in its production and its geographical origin. Consequently, these factors will influence on its commercial value [1]. Wine is a complex mixture which besides water and ethanol contains many organic compounds such as polyphenols, flavonoids [2], inorganic compounds minority among other classes of compounds. They turns wine into a product appreciated all over the world and considered a product with beneficial health properties, among other factors, by its antioxidant power [3].

Information on wine composition can be accessed by instrumental analysis techniques and used as a fingerprint for authenticity of a wine respect to grape variety or even of its geographical origin [4]. The wine fingerprint information can be useful in various fields like economy, plant physiology study, health and forensic purposes [5].

Food fingerprint approaches, also known as non-target analysis, have become a powerful tool for quality control of many products, for example, edible oil [6], fruit juice [7], alcoholic beverage [8], milk powder [9] among others [10]. These methodologies have been developed for different purposes, like to vouch authenticity brand or geographical origin [11,12] to detect presence of adulterants compounds [13].

Hyphenated techniques as liquid chromatography with diode array detection (DAD) or MS provide methodologies with potential for food fingerprint development. Recently, capillary electrophoresis (CE) has emerged as a powerful analytical tool able to promote, in some cases, better separation than traditional HPLC. As discussed by Gomez et al., in his recent review paper, the main advantage of CE, when compared to traditional methods to analyze wine samples is that almost no pretreatment of the sample is needed beyond a simple filtration [14]. The latter fact represents a major advantage from the viewpoint of green chemistry [15].

CE with DAD instrument furnishes second-order data which are able to extract important analytical information about the sample [16]. This type of data can be suitably modeled with mathematical algorithms giving loadings profiles which can be associated with pure compounds present in the sample even in the presence of strongly overlapped peaks [17].

The mentioned mathematical algorithms are known as multiway methods [18], being some of the most popular

Correspondence: Héctor C. Goicoechea, Laboratorio de Desarrollo Analítico y Quimiometría (LADAQ), Cátedra de Química Analítica I, Facultad de Bioquímica y Ciencias Biológicas, Universidad Nacional del Litoral-CONICET, Ciudad Universitaria, Santa Fe, S3000ZAA
E-mail: hgoico@fbcb.unl.edu.ar

*jcaminia@exactas.unlpam.edu.ar (J.M. Camiña)

Colour Online: See the article online to view Figs. 1–4 in colour.

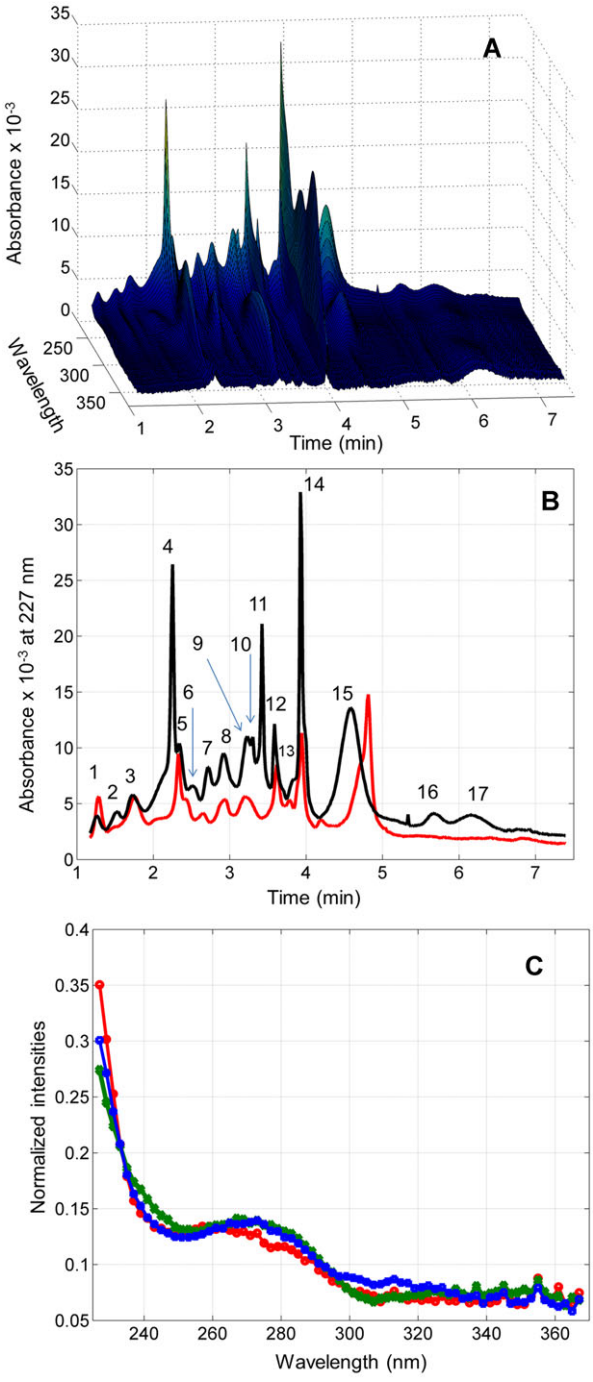

Figure 1. CE-DAD data: (A) typical landscape; (B) electropherogram recorded at 227 nm for Chardonnay (solid red line), Sauvignon Blanc (Blue dotted line) and Torrontés (cross black line); (C) spectral profile.

parallel factors analysis (PARAFAC) [19], multivariate curve resolution with alternating least squares (MCR-ALS) [20] and Tucker methods [21]. The latter is probably the least known, certainly for generating more complex models which have non-trivial interpretation. On the other hand, a Tucker method variant known as Tucker3 presents a great advantage: the ability to model properly data with certain drawbacks like remarkable peak misalignment and shape deformation in a data mode associated with deficiency rank in the other one. This drawbacks, usually found when modeling CE-DAD data, can represent limiting factors to traditional methods [22].

Ledyard Tucker, working with psychometric data, developed a series of methods which are known as Tucker methods [23]. These methods are nowadays known as multidimensional principal component analysis (PCA) or multiway PCA [24]. The Tucker3 methods, when applied to three way arrays $\boldsymbol{X}$ ($I \times J \times K$), with elements x_{ijk}, produces the loadings matrix **A** ($I \times L$), **B** ($J \times M$) and **C** ($K \times N$), where a_{il}, b_{jm} and c_{kn} are the elements of the loadings matrices **A**, **B** and **C**, respectively. The number of columns (L, M and N) in the loadings matrices corresponds to the number of factors in each mode. Interestingly, unlike of traditional multiway methods, in Tucker-3 decomposition different amounts of factors in each mode are permitted (i.e. $L \neq M \neq N$), being this feature of great versatility. The mathematical expression representing the Tucker3 model is given in Eq. (1).

$$\chi_{ijk} = \sum_{l=1}^{L}\sum_{m=1}^{M}\sum_{n=1}^{N} a_{il} b_{jm} c_{kn} g_{lmn} + e_{ijk} \quad (1)$$

where e_{ijk} are the elements of three-way array $\boldsymbol{E}$ ($I \times J \times K$) containing unmolded information by Tucker3 and g_{lmn} are the elements of three-way array $\boldsymbol{G}$ ($L \times M \times N$) called core. The core elements are the magnitude of the interaction between factors in different modes. Another striking difference of Tucker-3 method with respect to other multiway methods is that $\boldsymbol{G}$ is non-diagonal [24, 25]. This means that there is interaction between factors.

Let suppose a Tucker3 model with complexity 3, 4, 3 ($L = 3$, $M = 4$ and $N = 3$), where the element g_{121} has very low value (near zero), this means that the interaction between the first factor in mode 1, second factor in mode 2 and first factor in mode 3 is no significant. On the other hand, if g_{221} has a high value, the interaction between second factor in mode 1, second factor in mode 2 and first factor in mode 3 has significant importance for the model. These cross-interactions between factors present in Tucker3 models provide flexibility but increase complexity, becoming the interpretation in a non-trivial fact [24].

As in other multiway methods, an important step is the factor number determination, in this case for each mode. Several approaches can be used: chemical information about the system, cross validation and the increase in variance explained in terms of the number of factors used. A useful method for choosing the number of components in Tucker3 analysis, which was implemented herein, is based on inspection of the eigenvalues of the matrices $\boldsymbol{X}_a$ ($I \times JK$), $\boldsymbol{X}_b$ ($J \times IK$) and $\boldsymbol{X}_c$ ($K \times IJ$), obtained with frontal planes of $\boldsymbol{X}$ ($I \times J \times K$) [24–26].

In the present work, an investigation of white wine samples produced from three varieties of Argentinean grapes, namely Chardonnay (Char), Sauvignon Blanc wine (Sau) and Torrontés (Tor) is presented. Information on the composition

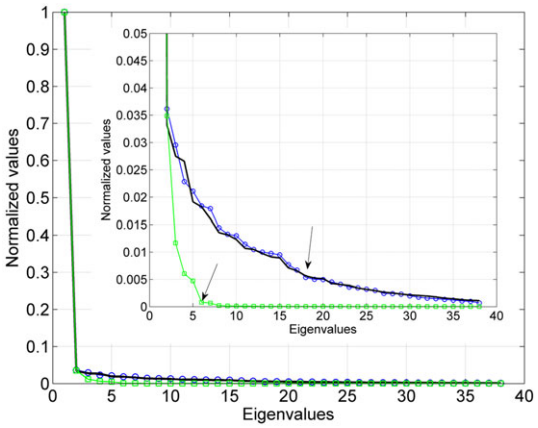

Figure 2. Eigenvalues plot of the frontal plane of *X*, mode 1(circle line), mode 2 (solid line) and mode 3 (square line).

of the white wine samples was accessed using CE-DAD data, modeled by Tucker3 method for the purpose of identifying loadings profiles that may be a fingerprint of the white wine samples with respect to grape variety. In addition, an investigation of the discriminating power of the CE-DAD data by linear discriminant analysis (LDA) and Kernel linear discriminant analysis (K-LDA).

2 Materials and methods

2.1 Samples

Thirty-eight samples of commercial white wine from four wine-producing provinces of Argentina (Mendoza, San Juan, Salta, and Rio Negro) were included in this study: 11 Torrontés wine (from Mendoza, San Juan, Salta, and Río Negro), 14 Chardonnay wine (from Mendoza and San Juan), and 13 Sauvignon Blanc wine (from Mendoza, San Juan, and Río Negro). Wines samples were selected from the 2011 to 2013 vintages. The alcoholic content ranged from 12.2 to 13.8% vol/vol ethanol. All were bought from a local supermarket.

2.2 CE-DAD measurements

All experiments were conducted on a CE system (Agilent Technologies, Waldbronn, Germany) equipped with a DAD. An uncoated fused silica capillary of 40 cm total length (31.5 cm effective length) and 75 μm inner diameter (MicroSolv Technology Corporation, Eatontown, NJ, USA) was used. Separation was performed by applying a voltage of 24 kV and with a typical current of approximately 80 μA. The cartridge was maintained at 25.0°C. The electropherograms were recorded during 10 min, and the second-order data were obtained by recording UV spectra between 189 and 401 nm each 2 nm at 0.3 s steps. The hydrodynamic injection was performed in the positive electrode of the capillary by applying a pressure of 40 mbar for 8 s.

To condition and activate the capillary, daily rinses were performed with 1.0 mol/L NaOH, ultrapure water, and BGE for 10 min each. The BGE consisted of a mixture of Na2B4O7 with a concentration of 10 mmol/L and SDS with a concentration of 20 mmol/L, adjusted to pH 9.40.

To remove substances adsorbed on the capillary wall, the capillary was flushed between runs with 1.0 mol/L NaOH, ultrapure water, and BGE for 3 min each. At the end of the day, the capillary was washed with 1.0 mol/L NaOH (5 min) and ultrapure water (5 min) and then air-dried for 3 min.

2.3 Data analysis and software

Initially, the working range was selected by visual inspection of CE-DAD arrays and it was maintained only informative region. The working region corresponds to CE-DAD matrices with size 421 elution times (from 1.17 to 7.39 min) x 71 wavelengths (from 227 to 367 nm). Following, these matrices were arranged in a three way array *X* of size: 38 samples x 421 times x 71 wavelengths.

Three-way array decomposition was carried out by Tucker3 using N-way toolbox [27] available in http://www.models.life.ku.dk/nwaytoolbox in MatLab® environmental [28]. The model complexity in each instrumental mode, was based on inspection of the eigenvalues of the matrices *X*a (*I* x *JK*), *X*b (*J* x *IK*) and *X*c (*K* x *IJ*), obtained with frontal planes of *X* (*I* x *J* x *K*). The Tucker decomposition output information was used in fingerprint analysis and the elements of the A matrix were used for discrimination propose by LDA and Kernel-LDA.

3 Results and discussion

3.1 CE-DAD data

In Fig. 1A a typical CE-DAD landscape for one type of white wine investigated in this study is displayed. As can be seen, the CE-DAD data has many overlapping peaks corresponding to the complex mixture of chemical compounds which are present in the white wine. The latter fact can be better appreciated by visual inspection of Fig. 1B, which displays the electropherograms recorded at 227 nm for two Chardonnay wine samples. As can be seen, a remarkable peak misalignment and shape deformation in electrophoretic mode is produced.

In addtion, considering the electropherogram of the Chardonnay wine samples (solid black line) in Fig. 1B, for example, seventeen peaks can be identified by visual inspection, disregarding the possibility of full co-elution. But, when examining the spectra corresponding to the 17 peaks in the maximum absorbance, several peaks have similar spectra, this is shown for the case of peak 3, 6 and 13 e.g. (see Fig. 1C). This is because many of the compounds in white wine has the same chromophores. this effect is exacerbated when comparing samples from different varieties of grapes.

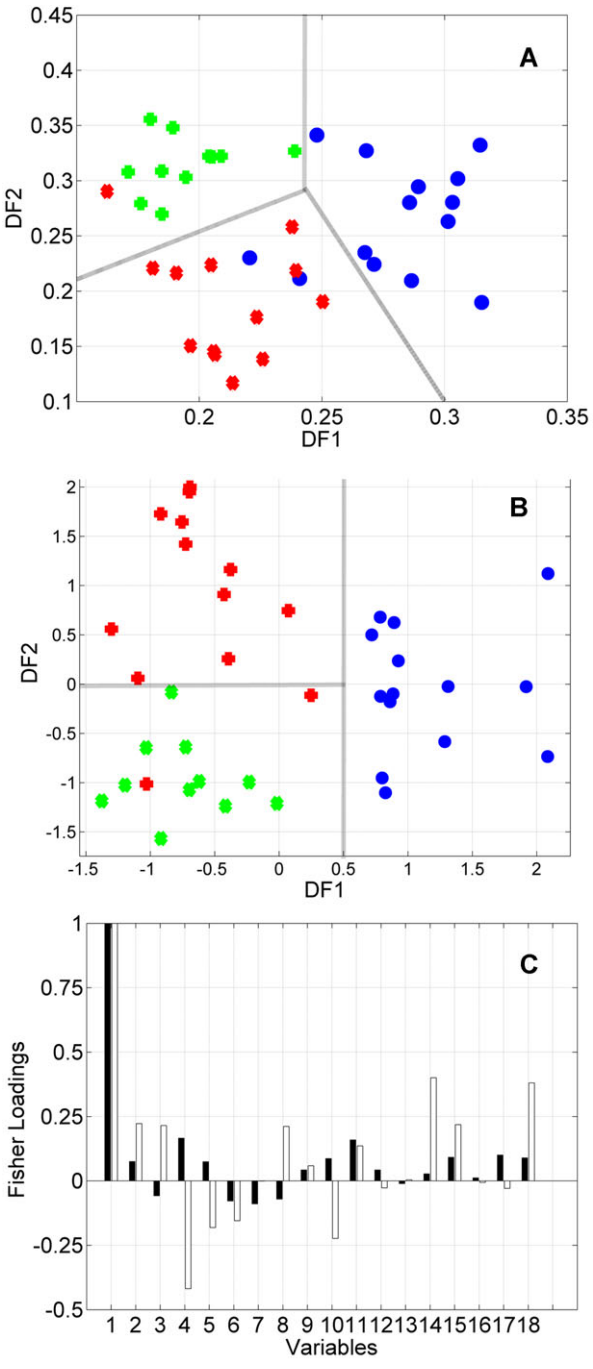

Figure 3. LDA results: (A) linear discriminant function plot (DF1 x DF2), (B) Kernel discriminant function plot (DF1 x DF2) and (C) Fisher loading plot, DF1 (black bars) and DF2 (white bars). Chardonnay (blue circle), Sauvignon Blanc (x red) and Torrontés (green cross).

From the point of view of chemometrics, most multiway methods assume that each chemical compound is associated with an instrumental profile (electropherogram and spectrum in this case), which is invariable in shape and position. Peak misalignment of the samples to sample allows a single chemical compound, has different retention times and electrophoretic profile in different samples. This peculiarity makes the data nontrilinear, precluding the use of trilinear algorithms as PARAFAC.

An alternative would be modeling with MCR-ALS (with matrix augmentation in the column wise mode), which can solve the problem of peak misalignment and shape deformation in electrophoretic mode. But for this to be possible, spectral profiles should be different from each other, which does not occur in this case. The consequence of this similarity between the spectra of different compounds is that the CE-DAD matrix data will be rank deficient, which constitutes a problem of considerable complexity from the data modeling point of view. MCR-ALS can not provide good solutions for data presenting peak misalignmen, shape deformation and rank deficiency, simultaneously. For these reasons, the Tucker3 method, which allows using a different number of factors in each mode (see above), have been chosen for modeling the present data.

3.2 Tucker3 analysis

Due to the high data complexity comented above, Tucker3 algorithm was chosen to model CE-DAD matrices. Initially, the number of factors (or model complexity) has been defined by inspection of the eigenvalues (see Fig. 2) of the matrices *X*a (38×29891), *X*b (421×15998) and *X*c (71×2698), obtained from frontal planes of *X* (38×421×71).

As can be appreciated in Fig. 2, two factors are suggested in all modes. However, the model (2 2 2) explains only about 77% of data variance. This suggests that a increased number of factors should be used in order to build a model which explains a larger percent of the variance. Thus, a visual inspection of the zoom in Fig. 2 suggests that the number of eigenvalues selected could be changed to 18, 18 and 6, for modes 1, 2 and 3, respectively.

The large number of factors in modes 1 and 2 agrees well with the complexity of the CE-DAD data, in which several peaks appear in electropherograms. In addition, many of these peaks corresponds to compounds with higly similar spectra. The latter fact explains that only six factors are needed in mode 3. Interestingly, the complex model which is represented as (18 18 6) corresponds to 95% of the variance of the data.

Tucker3 was implemented on the CE-DAD data employing the number of factors indicated above, and imposing an unique constraint: non-negativity in all modes. Although the concentration profiles obtained by CE-DAD data decomposition must be unimodal, in this case the unimodality was not fulfilled, certainly due to remarkable peak misalignment and shape deformation. When this constriant was used, the Tucker3 algorithm did not achieve convergence. As output of Tucker3 decomposition three matrices were obtained, containing the loadings *A*(38 × 18), *B*(421 × 18) and *C*(6 × 71). They correspond to instrumental modes concentration, electropherogram and spectra profiles, respectively. Besides, a *G* core (18×18×6) is obtained after the modeling, whose

Table 1. Significant core elements used for white wine discrimination purpose

Factors in mode 2 (electropherograms)			Factors in mode 3 (spectral)			
	1	2	3	4	5	6
1	**0.54**	0.29	0.04	0.05	0.10	−0.01
2	0.43	−0.42	0.24	−0.04	0.06	0.00
3	0.10	**−1.00**	0.00	−0.34	−0.21	−0.02
4	−0.29	−0.01	0.05	0.08	−0.09	0.10
5	−0.23	−0.08	−0.36	−0.13	−0.32	−0.02
6	**−0.57**	0.32	0.04	−0.05	−0.13	−0.06
7	0.40	**0.68**	−0.02	−0.03	0.07	−0.13
8	0.22	−0.24	−0.09	−0.06	−0.12	0.01
9	0.01	−0.02	0.02	0.03	0.03	0.00
10	0.15	−0.17	0.01	0.00	0.04	−0.02
11	0.25	0.30	0.02	0.26	0.19	0.11
12	0.35	0.28	0.21	0.11	0.25	0.04
13	−0.13	0.30	0.11	0.01	0.05	−0.06
14	**0.65**	0.11	0.06	0.17	0.23	0.01
15	0.16	0.14	0.03	0.03	0.11	−0.03
16	0.18	−0.36	−0.06	−0.07	−0.08	0.06
17	0.14	−0.04	−0.18	−0.07	−0.17	0.00
18	−0.09	−0.15	−0.20	−0.01	−0.13	0.00

elements correspond to the magnitude of the interaction between factors in different modes.

After that, a linear discrimant analysis performed using the information regarding the samples contained in the A Tucker3 loading matrix. The obtained results are shown in the scatter plot of discriminant functions DF1 vs DF2 (see Fig. 3A). As can be seen in the scatter plot suggests that, the CE-DAD data contain the appropriate information to discriminate different types of Argentine white wine with respect to grape variety. However due to the matrix complexity, wine samples discrimination can be improved using non-linear approaches. Thus, A (Tucker output) matrix was projected in a gaussian space to obtain the Kernel matrix (K) sized 38×38. Using the new matrix K, was carried out a linear discriminant analysis. Scatter plot of discriminant functions DF1 vs DF2 by Kernel-LDA is displayed in Fig. 3B.

As can you be seen, in both plots, white wine samples form clusters according to the type of grape, and it is possible to note that the Fisher scores of the Torrontés wines has lower scattering. Moreover, Fisher scores corresponding to Chardonnay and Sauvignon Blanc wines present high dispersion when compared to Torrontés scores. It can also be observed that wine Chardonnay and Sauvignon Blanc wines samples show a small overlapping in linear model, in other hand this overlap is resolved by non-linear approach.

Also with respect to the linear discriminant analysis, it is possible to observe that the first discriminant function (DF1) is associated with discrimination of Chardonnay wine samples owing to this variety of wine presents the larger values of DF1. On the other hand discrimination of samples of the type Sauvignon Blanc and Torrontés is mostly based on the second discriminant function (DF2).

The Fisher loading plot for DF1 (black bars) and DF2 (white bars) can be appreciated in Fig. 3B. Note that the input data (variables) to the LDA model was the A(38 × 18) matrix obtained in Tucker3 decomposition. Thus, each column in A has a Fisher loading in DF1 and a Fisher loading in DF2. A variable with high value of the Fisher loading indicates a high discriminant power. It is valid to remember that a Fisher loading has a similar interpretation than a PCA loading.

As can be seen in the Fig. 3B, the largest contribution in DF1 and DF2 corresponds to the first variable (the first A column). In other words, this means that Tucker factor 1 (corresponding to the first A column) is the most significant one to discriminate wine the Chardonnay, Torrontés and Sauvignon Blanc samples.

As previously mentioned, the core elements represent the magnitude of the interaction between factors in different modes. Therefore, Tucker3 factors in mode 2 (electropherograms) and mode 3 (spectra) presenting significant interaction as the factor 1 in concentration mode are also related to discrimination of white wine samples. An inspection of the *G* values reveals the Tucker3 factors in the electropherogram and spectral modes with significant interaction with the factor 1 (concentration mode). In Table 1 are shown the tensor *G* (l × m × n) normalized values corresponding to the slice 1 × m × n; were considered significant the triads with g(lmn) value greater than or equal to 0.5.

As can be seen in Table 1, the highlighted values correspond to the triads g1,1,1; g1,1,4; g1,1,14; g1,2,3 and g1,2,7. In other words, this means that in electropherogram mode are important the factors 1, 3, 4, 7 and 14. Moreover in the spectral mode only the factors 1 and 2 show greater contribution for discrimination proposes.

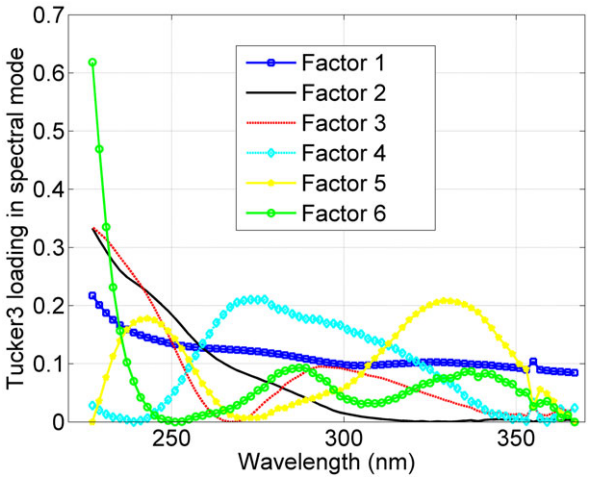

Figure 4. Tucker3 loading profiles in spectral mode.

Loading profiles corresponding to the six factors extracted in the spectral mode are displayed in Fig. 4. The loadings vectors are directly related to the pure spectra of constituents of white wine samples. Interestingly the profiles represented in Fig. 4, retrieved by the Tucker3 algorithm, show high agreement with white wine constituents UV-VIS spectra profiles reported in literature [29–31]. In particular, the factors 1 and 2 (represented by the blue and black solid lines, respectively) are directly linked to varietal discrimination of Argentinean white wine samples. Comparing these two profiles with spectral profiles shown in the literature [29–31] it is possible to see remarkable similarity with the spectra profiles of the phenolic compounds, rutin and quercetin reported in [30].

It is known that phenolic compounds, as well as, gallic acid, protocatechuic acid, caffeic acid, salicylic acid, catechin, quercetin, resveratrol, rutin among others, contribute in an important manner to wine characteristics like taste and bitterness, for example. In addition, the same chemometric studies described above were performed to assess vintage discrimination in white wines. However, the phenolic composition has shown to have little influence on the vintage in white wines. Therefore, the grape variety was the largest contributing factor to the phenolic composition of Argentinean wines. Thus, it was concluded that concentration of phenolic compounds can vary of wine to wine as a function of several factors, one of the most important is the grape type, indicating the potential application of this technique for variety establishment purposes.

This fact explains why Tucker3 factors related to this kind of compounds are precisely those containing information able of discriminating Argentinean white wine with respect to grape variety.

4 Concluding remarks

In this work it was shown that valuable information about the grape variety employed in the production of an Argentinean white wine can be accessed through CE-DAD data modeled by three way data decomposition based on the versatile Tucker3 algorithm. This approach overcomes the drawbacks originated when using such complex data. Despite that some factors can limit the precision of the classification models, such as the number of samples and the similarities between some wines due to climate, soil, or other characteristics, this modeling allows discriminating the white wine samples from Argentina with respect to grape variety.

The authors are grateful to UNL, CONICET, ANPCyT, CNPq (research fellowships), and UNLPam for financial support.

The authors declare that they have no competing interests.

5 References

[1] Fanzone, M., Peña-Neira A., Gil, M., Jofré, V., Assof, M., Zamora, F., *Food Res. Int.* 2012, *45*, 402–414.

[2] Moreno, J., Peinado, R., *Enological Chemistry*, Academic Press, Spain 2012.

[3] Mena, P., Gironés-Vilaplana, A, Martí, N., García-Viguera, C., *Food Chem.* 2012, *133*, 108–115.

[4] Langstaff, S. A., in: Kilcast, D., (Ed.), *Sensory Quality Control in the Wine Industry*, CRC Press, USA 2010, pp. 236–260.

[5] Riedl, J., Esslinger, S., Fauhl-Hassek, C., *Anal. Chim. Acta* 2015, *885*, 17–32.

[6] Bagur-González, M. G., Pérez-Castaño, E., Sánchez-Viñas, M., Gázquez-Evangelista, D., *J. Chromatogr. A* 2015, *1380*, 64–70.

[7] Lerma-García, M. J., D'Amato, A., Simó-Alfonso, E. F., Giorgio Righetti, P., Fasoli, E., *Food Chem.* 2016, *196*, 739–749.

[8] Galano, E., Imbelloni, M., Chambery, A., Malorni, A., Amoresano, A., *Food Res. Int.* 2015, *72*, 106–114.

[9] Rodrigues Júnior, P. H., de Sá Oliveira, K., Rocha de Almeida, C. E., Cappa De Oliveira, L. F., Stephani, R., da Silva Pinto, M., Fernandes de Carvalho, A., Tuler Perrone, T., *Food Chem.* 2016, *196*, 584–588.

[10] Carrera, M., Cañas, B., Gallardo, J. M., in: *Proteomics Tools for Food Fingerprints: Addressing New Food Quality and Authenticity Challenges*, Academic Press, New York 2014, pp. 201–222.

[11] Lohumi, S., Lee, S., Lee, H., Cho, B., *Trends Food Sci. Tech.* 2015, *46*, 85–98.

[12] Goodarzi, M., Russell, P. J., Vander Heyden, Y., *Anal. Chim. Acta* 2013, *804*, 16–28.

[13] Knolhoff, A. M., Croley, T. R., *J. Chromatogr. A* 2016, *1428*, 86–96.

[14] Gomez, F. J. V., Monasterio, R. P., SotoVargas, V. C., Silva, M. F., *Electrophoresis* 2012, *33*, 2240–2252.

[15] Fegade, S. L., Trembly, J. P., *Ultrason. Sonochem.* 2015, In Press.

[16] Escandar, C. M., Goicoechea, H. C., Muñoz de la Peña, A., Olivieri, A. C., *Anal. Chim. Acta* 2014, *806*, 8–26.

[17] Arancibia, J. A., Damiani, P. C., Escandar, G. M., Ibañez, G. A., Olivieri, A. C., *J. Chromatogr. B* 2012, *910*, 22–30.

[18] Olivieri, A.C., *Anal. Chem.* 2008, *80*, 5713–5720.

[19] Murphy, K. R., Stedmon, C. A., Graeberc, D., Bro, R., *Anal. Methods* 2013, *5*, 6557–6566.

[20] Parastar, H., Tauler, R., *Anal. Chem.* 2014, *86*, 286–297.

[21] Kompany-Zareha, M., Akhlaghia, Y., Bro, R., *Anal. Chim. Acta* 2012, *723*, 18–26.

[22] Bortolato, S. A., Arancibia, J. A., Escandar, G. M., Olivieri, A. C., *Chemometr. Intell. Lab.* 2010, *101*, 30–37.

[23] Soares, P. K., Bruns, R. E., Scarminio, I. S., *Anal. Chim. Acta* 2012, *736*, 36–44.

[24] Ten Berge, J. M. F., *J. Chemometrics* 2004, *18*, 17–21.

[25] Ten Berge, J. M. F., Smilde, A. K., *J. Chemometrics* 2002, *16*, 609–612.

[26] Smilde, A., Bro, R., Geladi, P., *Multi-way Analysis with Applications in the Chemical Sciences*, John Wiley & Sons Ltd, England 2010.

[27] Andersson, C. A., Bro, R., *Chemometr. Intell. Lab.* 2000, *52*, 1–4.

[28] MATLAB. (2010). Matlab 7.10. Natick Massachusetts: The Math Works Inc.

[29] Cejudo-Bastante, M. J., Pérez-Cohelo, M. S., Hermosín-Gutierrez, I., *J. Agric. Food Chem.* 2010, *58*, 11483–11492.

[30] Gorinstein, S., Weisz, M., Zemser, M., Tilis, K., Stiller, A., Flam, Gat, Y., *J. Ferment. Bioeng.* 1993, *75*, 115–120.

[31] Zhang, A., Wan, L., Wu, C., Fang, Y., Han, G., Li, H., Zhang, Z., Wang, H., *Molecules* 2013, *18*, 14241–14257.

